Striking Antibody Evasion Manifested by the Omicron Variant of SARS-CoV-2

Lihong Liu[1]*, Sho Iketani[1,2]*, Yicheng Guo[1]*, Jasper F-W. Chan[3, 4]*, Maple Wang[1]*, Liyuan Liu[5]*, Yang Luo[1], Hin Chu[3,4], Yiming Huang[5], Manoj S. Nair[1], Jian Yu[1], Kenn K-H. Chik[4], Terrence T-T. Yuen[3], Chaemin Yoon[3], Kelvin K-W. To[3,4], Honglin Chen[3,4], Michael T. Yin[1,6], Magdalena E. Sobieszczyk[1,6], Yaoxing Huang[1], Harris H. Wang[5], Zizhang Sheng[1], Kwok-Yung Yuen[3,4], David D. Ho[1,2,6^]

[1]Aaron Diamond AIDS Research Center, Columbia University Vagelos College of Physicians and Surgeons, New York, NY 10032, USA

[2]Department of Microbiology and Immunology, Columbia University Vagelos College of Physicians and Surgeons, New York, NY 10032, USA

[3]State Key Laboratory of Emerging Infectious Diseases, Carol Yu Centre for Infection, Department of Microbiology, Li Ka Shing Faculty of Medicine, The University of Hong Kong, Pokfulam, Hong Kong Special Administrative Region, China

[4]Centre for Virology, Vaccinology and Therapeutics, Hong Kong Science and Technology Park, Hong Kong Special Administrative Region, China

[5]Department of Systems Biology, Columbia University Vagelos College of Physicians and Surgeons, New York, NY 10032, USA

[6]Division of Infectious Diseases, Department of Medicine, Columbia University Vagelos College of Physicians and Surgeons, New York, NY 10032, USA

* These authors contributed equally

^ Address correspondence to David D. Ho (dh2994@cumc.columbia.edu, 212-304-6101, 701 W 168th St, 11th Floor, New York, NY 10032)

Word count: 3309

Abstract

The Omicron (B.1.1.529) variant of SARS-CoV-2 was only recently detected in southern Africa, but its subsequent spread has been extensive, both regionally and globally[1]. It is expected to become dominant in the coming weeks[2], probably due to enhanced transmissibility. A striking feature of this variant is the large number of spike mutations[3] that pose a threat to the efficacy of current COVID-19 vaccines and antibody therapies[4]. This concern is amplified by the findings from our study. We found B.1.1.529 to be markedly resistant to neutralization by serum not only from convalescent patients, but also from individuals vaccinated with one of the four widely used COVID-19 vaccines. Even serum from persons vaccinated and boosted with mRNA-based vaccines exhibited substantially diminished neutralizing activity against B.1.1.529. By evaluating a panel of monoclonal antibodies to all known epitope clusters on the spike protein, we noted that the activity of 18 of the 19 antibodies tested were either abolished or impaired, including ones currently authorized or approved for use in patients. In addition, we also identified four new spike mutations (S371L, N440K, G446S, and Q493R) that confer greater antibody resistance to B.1.1.529. The Omicron variant presents a serious threat to many existing COVID-19 vaccines and therapies, compelling the development of new interventions that anticipate the evolutionary trajectory of SARS-CoV-2.

Main text

The COVID-19 pandemic rages on, as the causative agent, SARS-CoV-2, continues to evolve. Many diverse viral variants have emerged (**Fig. 1a**), each characterized by mutations in the spike protein that raise concerns of both antibody evasion and enhanced transmission. The Beta (B.1.351) variant was found to be most refractory to antibody neutralization[4] and thus compromised the efficacy of vaccines[5-7] and therapeutic antibodies. The Alpha (B.1.1.7) variant became dominant globally in early 2021 due to an edge in transmission[8] only to be replaced by the Delta (B.1.617.2) variant, which exhibited even greater propensity to spread coupled with a moderate level of antibody resistance[9]. Then came the Omicron (B.1.1.529) variant, first detected in southern Africa in November 2021[3,10,11] (**Fig. 1a**). It has since spread rapidly in the region, as well as to over 60 countries, gaining traction even where the Delta variant is prevalent. The short doubling time (2-3 days) of Omicron cases suggests it could become dominant soon[2]. Moreover, its spike protein contains an alarming number of >30 mutations (**Fig. 1b and Extended Data Fig. 1**), including at least 15 in the receptor-binding domain (RBD), the principal target for neutralizing antibodies. These extensive spike mutations raise the specter that current vaccines and therapeutic antibodies would be greatly compromised. This concern is amplified by the findings we now report.

Serum neutralization of B.1.1.529

We first examined the neutralizing activity of serum collected in the Spring of 2020 from COVID-19 patients, who were presumably infected with the wild-type SARS-CoV-2 (see Methods). Samples from 10 individuals were tested for neutralization against both D614G (WT) and B.1.1.529 pseudoviruses. While robust titers were observed against D614G, a significant drop (>32-fold) in ID_{50} titers was observed against B.1.1.529, with only 2 samples showing titers above the limit of detection (LOD) (**Fig. 1c and Extended Data Fig. 2a**). We then assessed the neutralizing activity of sera from individuals who received one of the four widely used COVID-19 vaccines: BNT162b2 (Pfizer), mRNA-1273 (Moderna), Ad26.COV2.S (Johnson & Johnson), and ChAdOx1 nCoV-19 (AstraZeneca) (see Methods and **Extended Data Table 1**). In all cases, a substantial loss in neutralizing potency was observed against B.1.1.529 (**Fig. 1d and Extended Data Fig. 2b-f**). For the two mRNA-based vaccines, BNT162b2 and mRNA-1273, a >21-fold and >8.6-fold decrease in ID_{50} was seen, respectively. We note that, for these two groups, we

76 specifically chose samples with high titers such that the fold-change in titer could be better
77 quantified, so the difference in the number of samples having titers above the LOD (6/13 for
78 BNT162b2 versus 11/12 for mRNA-1273) may be favorably biased. Within the Ad26.COV2.S
79 and ChAdOx1 nCOV-19 groups, all samples were below the LOD against B.1.1.529, except for
80 two Ad26.COV2.S samples from patients with a previous history of SARS-CoV-2 infection (**Fig.**
81 **1d**). Collectively, these results suggest that individuals who were previously infected or fully
82 vaccinated remain at risk for B.1.1.529 infection.
83
84 Booster shots are now routinely administered in many countries 6 months after full vaccination.
85 Therefore, we also examined the serum neutralizing activity of individuals who had received three
86 homologous mRNA vaccinations (13 with BNT162b2 and 2 with mRNA-1273). Every sample
87 showed lower activity in neutralizing B.1.1.529, with a mean drop of 6.5-fold compared to WT
88 (**Fig. 1d**). Although all samples had titers above the LOD, the substantial loss in activity may still
89 pose a risk for B.1.1.529 infection despite the booster vaccination.
90
91 We then confirmed the above findings by testing a subset of the BNT162b2 and mRNA-1273
92 vaccinee serum samples using authentic SARS-CoV-2 isolates: wild type and B.1.1.529. Again,
93 a substantial decrease in neutralization of B.1.1.529 was observed, with mean drops of >6.0-fold
94 and >4.1-fold for the fully vaccinated group and the boosted group, respectively (**Fig. 1e**).
95
96 **Monoclonal antibody neutralization of B.1.1.529**
97 To understand the types of antibodies in serum that lost neutralizing activity against B.1.1.529, we
98 assessed the neutralization profile of 19 well-characterized monoclonal antibodies (mAbs) to the
99 spike protein, including 17 directed to RBD and 2 directed to the N-terminal domain (NTD). We
100 included mAbs that have been authorized or approved for clinical use, either individually or in
101 combination: REGN10987 (imdevimab)[12], REGN10933 (casirivimab)[12], COV2-2196
102 (tixagevimab)[13], COV2-2130 (cilgavimab)[13], LY-CoV555 (bamlanivimab)[14], CB6 (etesevimab)[15],
103 Brii-196 (amubarvimab)[16], Brii-198 (romlusevimab)[16], and S309 (sotrovimab)[17]. We also
104 included other mAbs of interest: 910-30[18], ADG-2[19], DH1047[20], S2X259[21], and our antibodies 1-
105 20, 2-15, 2-7, 4-18, 5-7, and 10-40[22-24]. The footprints of mAbs with structures available were
106 drawn in relation to the mutations found in B.1.1.529 RBD (**Fig. 2a**) and NTD (**Fig. 2b**). The risk

107 to each of the 4 classes[25] of RBD mAbs, as well as to the NTD mAbs, was immediately apparent.
108 Indeed, neutralization studies on B.1.1.529 pseudovirus showed that 18 of the 19 mAbs tested lost
109 neutralizing activity completely or partially (**Fig. 2c and Extended Data Fig. 3**). The potency of
110 class 1 and class 2 RBD mAbs all dropped by >100-fold, as did the more potent mAbs in RBD
111 class 3 (REGN10987, COV2-2130, and 2-7). The activity of S309 declined modestly, whereas
112 Brii-198 was spared. All mAbs in RBD class 4 lost neutralization potency against B.1.1.529 by at
113 least 10-fold, as did mAb directed to the antigenic supersite[26] (4-18) or the alternate site[23] (5-7) on
114 NTD. Strikingly, all four combination mAb drugs in clinical use lost substantial activity against
115 B.1.1.529, likely abolishing or impairing their efficacy in patients.
116
117 Approximately 10% of the B.1.1.529 viruses in GISAID[1] also contain an additional RBD mutation,
118 R346K, which is the defining mutation for the Mu (B.1.621) variant[27]. We therefore constructed
119 another pseudovirus (B.1.1.529+R346K) containing this mutation for additional testing using the
120 same panel of mAbs (**Fig. 2d**). The overall findings resembled those already shown in **Fig. 2c**,
121 with the exception that the neutralizing activities of S309 and Brii198 were further diminished or
122 abolished. In fact, the entire panel of antibodies was essentially rendered inactive against this
123 minor form of the Omicron variant.
124
125 The fold changes in IC_{50} of the mAbs against B.1.1.529 and B.1.1.529+R346K relative to D614G
126 are summarized in the first two rows of **Fig. 3a**. The remarkable loss of activity observed for all
127 classes of mAbs against B.1.1.529 suggest that perhaps the same is occurring in the serum of
128 convalescent patients and vaccinated individuals.
129
130 **Key mutations conferring antibody resistance**
131 To understand the specific B.1.1.529 mutations that confer antibody resistance, we next tested
132 individually the same panel of 19 mAbs against pseudoviruses for each of the 34 mutations
133 (excluding D614G) found in B.1.1.529 or B.1.1.529+R346K. Our findings not only confirmed the
134 role of known mutations at spike residues 142-145, 417, 484, and 501 in conferring resistance to
135 NTD or RBD (class 1 or class 2) antibodies[4] but also revealed several mutations that were
136 previously not known to have functional importance (**Fig. 3a and Extended Data Fig. 4**). Q493R
137 mediated resistance to CB6 (class 1) as well as to LY-CoV555 and 2-15 (class 2), findings that

138 could be explained by the abolishment of hydrogen bonds due to the long side chain of arginine
139 and induced steric clashes with CDRH3 in these antibodies (**Fig. 3b, left panels**). Both N440K
140 and G446S mediated resistance to REGN10987 and 2-7 (class 3), observations that could also be
141 explained by steric hindrance (**Fig. 3b, middle panels**). The most striking and perhaps unexpected
142 finding was that S371L broadly affected neutralization by mAbs in all 4 RBD classes (**Fig. 3a and**
143 **Extended Data Fig. 4**). While the precise mechanism of this resistance is unknown, in silico
144 modeling suggested two possibilities (**Fig. 3b, right panels**). First, in the RBD-down state,
145 mutating Ser to Leu results in an interference with the N343 glycan, thereby possibly altering its
146 conformation and affecting class 3 antibodies that typically bind this region. Second, in the RBD-
147 up state, S371L may alter the local conformation of the loop consisting of S371-S373-S375,
148 thereby affecting the binding of class 4 antibodies that generally target a portion of this loop (REF
149 10-40). It is not clear how class 1 and class 2 RBD mAbs are affected by this mutation.
150

151 **Evolution of antibody resistance of SARS-CoV-2 variants**

152 To gain insight into the antibody resistance of B.1.1.529 relative to previous SARS-CoV-2 variants,
153 we evaluated the neutralizing activity of the same panel of neutralizing mAbs against
154 pseudoviruses for B.1.1.7[8], B.1.526[28], B.1.429[29], B.1.617.2[9], P.1[30], and B.1.351[31]. It is evident
155 from these results (**Fig. 4** and **Extended Data Fig. 5**) that previous variants developed resistance
156 only to NTD antibodies and class 1 and class 2 RBD antibodies. Here B.1.1.529, with or without
157 R346K, has made a big mutational leap by becoming not only nearly completely resistant to class
158 1 and class 2 RBD antibodies, but also substantial resistance to both class 3 and class 4 RBD
159 antibodies. B.1.1.529 is now the most complete "escapee" from neutralization by currently
160 available antibodies.
161

162 **Discussion**

163 The Omicron variant struck fear almost as soon as it was detected to be spreading in South Africa.
164 That this new variant would transmit more readily has come true in the ensuing weeks[2]. The
165 extensive mutations found in its spike protein raised concerns that the efficacy of current COVID-
166 19 vaccines and antibody therapies might be compromised. Indeed, in this study, sera from
167 convalescent patients (**Fig. 1c**) and vaccinees (**Figs. 1d and 1e**) showed markedly reduced
168 neutralizing activity against B.1.1.529. These findings are in line with emerging clinical data on

169 the Omicron variant demonstrating higher rates of reinfection[11] and vaccine breakthroughs. In
170 fact, recent reports showed that the efficacy of two doses of BNT162b2 vaccine has dropped from
171 over 90% against the original SARS-CoV-2 strain to approximately 40% and 33% against
172 B.1.1.529 in the United Kingdom[32] and South Africa[33], respectively. Even a third booster shot
173 may not adequately protect against Omicron infection[32,34], but of course it is advisable to do so.
174 Vaccines that elicited lower neutralizing titers[35,36] are expected to fare worse against B.1.1.529.
175
176 The nature of the loss in serum neutralizing activity against B.1.1.529 could be discerned from our
177 findings on a panel of mAbs directed to the viral spike. The neutralizing activities of all four major
178 classes of RBD mAbs and two distinct classes of NTD mAbs are either abolished or impaired
179 (**Figs. 2c and 2d**). In addition to previously identified mutations that confer antibody resistance[4],
180 we have uncovered four new spike mutations with functional consequences. Q493R confers
181 resistance to some class 1 and class 2 RBD mAbs; N440K and G446S confer resistance to some
182 class 3 RBD mAbs; and S371L confers global resistance to many RBD mAbs via mechanisms that
183 are not yet apparent. While performing these mAb studies, we also observed that all the currently
184 authorized or approved mAb drugs are rendered weak or inactive by B.1.1.529 (**Figs. 2c and 3a**).
185 In fact, the Omicron variant that contains R346K seemingly flattens the antibody therapy
186 landscape for COVID-19 (**Fig. 2d and 3a**).
187
188 The scientific community has chased after SARS-CoV-2 variants for a year. As more and more
189 of them appeared, our interventions directed to the spike became increasingly ineffective. The
190 Omicron variant has now put an exclamation mark on this point. It is not too far-fetched to think
191 that this SARS-CoV-2 is now only a mutation or two away from being pan-resistant to current
192 antibodies, either monoclonal or polyclonal. We must devise strategies that anticipate the
193 evolutional direction of the virus and develop agents that target better conserved viral elements.

194 **Figure Legends**

195

196 **Fig. 1. Resistance of B.1.1.529 to neutralization by sera. a,** Unrooted phylogenetic tree of
197 B.1.1.529 with other major SARS-CoV-2 variants. **b,** Key spike mutations found in the viruses
198 isolated in the major lineage of B.1.1.529 are denoted. **c,** Neutralization of D614G and B.1.1.529
199 pseudoviruses by convalescent patient sera. **d,** Neutralization of D614G and B.1.1.529
200 pseudoviruses by vaccinee sera. Within the four standard vaccination groups, individuals that were
201 vaccinated without documented infection are denoted as circles and individuals that were both
202 vaccinated and infected are denoted as triangles. Within the boosted group, Moderna vaccinees are
203 denoted as squares and Pfizer vaccinees are denoted as diamonds. **e,** Neutralization of authentic
204 D614G and B.1.1.529 viruses by vaccinee sera. Moderna vaccinees are denoted as squares and
205 Pfizer vaccinees are denoted as diamonds. For all panels, values above the symbols denote
206 geometric mean titer and the numbers in parentheses denote the sample size. *P* values were
207 determined by using a Wilcoxon matched-pairs signed-rank test (two-tailed).

208

209 **Fig. 2. Resistance of B.1.1.529 to neutralization by monoclonal antibodies. a,** Footprints of
210 RBD-directed antibodies, with mutations within B.1.1.529 highlighted in cyan. Approved or
211 authorized antibodies are bolded. The receptor binding motif (RBM) residues are highlighted in
212 yellow. **b,** Footprints of NTD-directed antibodies, with mutations within B.1.1.529 highlighted in
213 cyan. The NTD supersite residues are highlighted in light pink. **c,** Neutralization of D614G and
214 B.1.1.529 pseudoviruses by RBD-directed and NTD-directed mAbs. **d,** Neutralization D614G and
215 B.1.1.529+R346K pseudoviruses by RBD-directed and NTD-directed mAbs.

216

217 **Fig. 3. Impact of individual mutations within B.1.1.529 against monoclonal antibodies. a,**
218 Neutralization of pseudoviruses harboring single mutations found within B.1.1.529 by a panel of
219 19 monoclonal antibodies. Fold change relative to neutralization of D614G is denoted, with
220 resistance colored red and sensitization colored green. **b,** Modeling of critical mutations in
221 B.1.1.529 that affect antibody neutralization.

222

223 **Fig. 4. Evolution of antibody resistance across SARS-CoV-2 variants.** Neutralization of SARS-
224 CoV-2 variant pseudoviruses by a panel of 19 monoclonal antibodies. Fold change relative to
225 neutralization of D614G is denoted.
226

Fig. 1

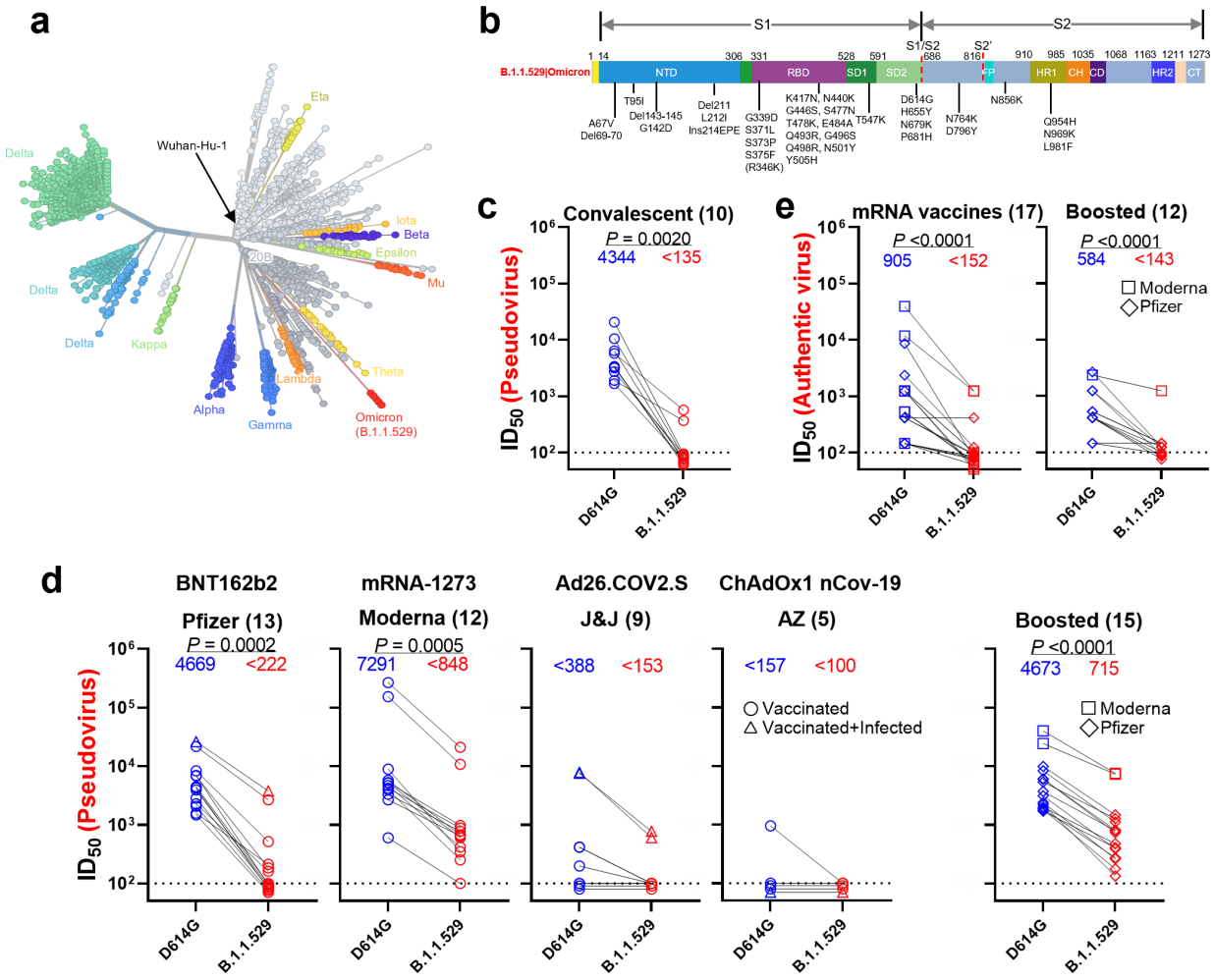
a
Wuhan-Hu-1
Eta
Delta
Iota
Beta
Epsilon
Mu
20B
Delta
Delta
Kappa
Theta
Lambda
Alpha
Gamma
Omicron
(B.1.1.529)
b
S1
S2
S1/S2
S2'
B.1.1.529|Omicron
NTD
RBD
SD1
SD2
FP
HR1
CH
CD
HR2
CT
A67V
Del69-70
T95I
Del143-145
G142D
Del211
L212I
Ins214EPE
G339D
S371L
S373P
S375F
(R346K)
K417N, N440K
G446S, S477N
T478K, E484A
Q493R, G496S
Q498R, N501Y
Y505H
T547K
D614G
H655Y
N679K
P681H
N764K
D796Y
N856K
Q954H
N969K
L981F
c
Convalescent (10)
P = 0.0020
4344
<135
ID50 (Pseudovirus)
D614G
B.1.1.529
e
mRNA vaccines (17)
P <0.0001
905
<152
Boosted (12)
P <0.0001
584
<143
Moderna
Pfizer
ID50 (Authentic virus)
d
BNT162b2
Pfizer (13)
P = 0.0002
4669
<222
mRNA-1273
Moderna (12)
P = 0.0005
7291
<848
Ad26.COV2.S
J&J (9)
<388
<153
ChAdOx1 nCov-19
AZ (5)
<157
<100
Vaccinated
Vaccinated+Infected
Boosted (15)
P <0.0001
4673
715
Moderna
Pfizer
ID50 (Pseudovirus)
D614G
B.1.1.529

227

228

Fig. 2

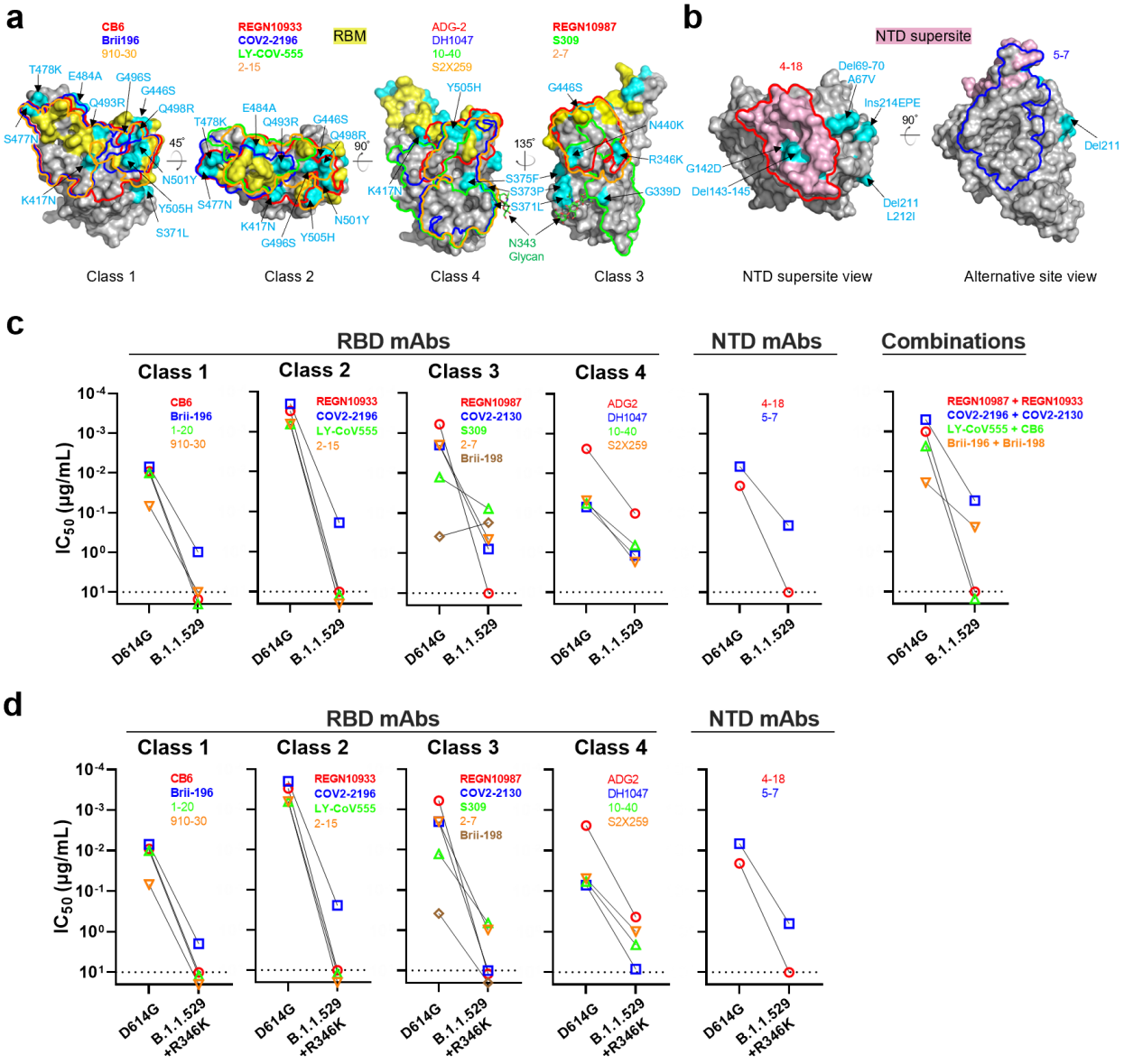
a
CB6
Brii196
910-30
REGN10933
COV2-2196
LY-COV-555
2-15
RBM
ADG-2
DH1047
10-40
S2X259
REGN10987
S309
2-7
T478K
E484A
G496S
G446S
Q493R
Q498R
S477N
N501Y
K417N
Y505H
S371L
45˚
90˚
135˚
Y505H
G446S
N440K
R346K
S375F
S373P
S371L
G339D
N343
Glycan
Class 1
Class 2
Class 4
Class 3
b
NTD supersite
4-18
Del69-70
A67V
Ins214EPE
G142D
Del143-145
Del211
L212I
5-7
Del211
NTD supersite view
Alternative site view
c
RBD mAbs
NTD mAbs
Combinations
Class 1
Class 2
Class 3
Class 4
CB6
Brii-196
1-20
910-30
REGN10933
COV2-2196
LY-CoV555
2-15
REGN10987
COV2-2130
S309
2-7
Brii-198
ADG2
DH1047
10-40
S2X259
4-18
5-7
REGN10987 + REGN10933
COV2-2196 + COV2-2130
LY-CoV555 + CB6
Brii-196 + Brii-198
IC50 (µg/mL)
D614G
B.1.1.529
d
RBD mAbs
NTD mAbs
Class 1
Class 2
Class 3
Class 4
B.1.1.529 +R346K

229

230

Fig. 3

a

Fold change in IC50 compared with WT	RBD mAbs																	NTD mAbs	
	Class 1				Class 2				Class 3					Class 4					
	CB6	Brii-196	1-20	910-30	REGN10933	COV2-2196	LY-CoV555	2-15	REGN10987	COV2-2130	S309	2-7	Brii-198	ADG-2	DH1047	10-40	S2X259	4-18	5-7
B.1.1.529	<-1000	-134	<-338	<-159	<-1000	-140	<-1000	<-1000	<-1000	-390	-6.1	-231	2.2	-43	-124	-11	-35	-125	-30
B.1.1.529 + R346K	<-761	-97	<-338	<-159	<-1000	-89	<-1000	<-1000	<-1000	<-988	-21	-109	<-32	-51	-167	-32	-16	-125	-33
A67V	1.1	1.0	-1.1	1.4	1.1	-1.0	1.1	1.1	1.1	1.2	-1.4	-1.1	-1.2	1.3	-1.3	-1.1	1.0	-1.6	-1.1
Del69-70	-1.4	-1.4	-1.6	-1.1	-1.8	-1.5	-1.4	-1.4	-1.7	-1.4	-2.2	-1.9	-2.3	-1.4	-3.3	-1.7	-1.3	-2.6	-9.4
T95I	-1.4	-2.0	-1.8	-1.7	-1.5	-1.6	-1.5	1.1	-2.0	-1.1	-2.3	-3.4	1.3	-2.5	-3.4	-1.9	-2.2	1.0	-9.5
G142D	-1.3	-1.4	-1.6	1.0	-1.6	-1.6	-1.7	-1.6	-1.9	-1.5	-2.9	-2.9	-1.5	-1.4	-2.8	-1.4	-1.5	<-125	-263
Del143-145	1.3	1.0	-1.2	1.4	1.3	1.6	1.3	1.5	1.1	-1.1	-1.9	1.2	-1.3	1.2	-2.0	-1.2	-1.2	<-125	-29
Del211	-2.4	-2.1	-1.6	-2.1	-1.5	-1.5	-1.4	-1.2	1.2	-1.2	-1.2	-1.3	-1.1	-1.9	-2.4	-1.6	-2.3	1.2	-9.1
L212I	-1.3	-1.8	-1.3	-1.6	-1.4	-1.4	-1.6	-1.3	-1.3	-1.4	-2.2	-1.9	-2.2	-1.7	-3.2	-2.0	-1.9	-7.2	-2.2
Ins214EPE	-2.4	-2.4	-2.2	-2.4	-2.8	-2.7	-2.3	-4.3	-3.0	-2.2	-3.0	-6.2	-2.7	-3.1	-2.9	-1.9	-3.3	-7.1	-15
G339D	-1.7	-1.6	-1.7	-1.4	-2.2	-1.7	-1.5	-1.4	-1.8	-1.6	-4.0	-1.9	-3.9	-1.6	-2.2	-1.5	-3.2	-4.5	-3.0
(R346K)	-1.5	-1.2	-1.3	1.0	-1.5	-1.3	-1.3	-1.4	-1.6	-2.9	-1.4	-1.0	-21	-1.1	-1.9	-1.2	-1.4	-1.4	-2.3
S371L	-19	-18	-15	-22	-10	-4.1	-2.9	-1.4	-25	-1.4	-12	-12	-17	-18	-49	-59	-23	-1.8	1.1
S373P	-1.9	-2.1	-1.6	-1.4	-1.9	-2.1	-2.0	-1.4	-1.9	-1.3	-2.3	-1.8	-2.5	-2.2	-5.1	-5.0	-2.8	-8.2	-5.0
S375F	1.7	1.6	1.6	1.5	2.1	1.9	1.9	2.6	1.2	1.5	-1.1	1.4	1.1	1.8	-1.8	-1.2	-1.6	-9.2	-1.6
K417N	<-761	-1.6	-2.3	<-158	-6.4	1.1	1.5	1.1	1.2	1.2	-1.8	1.5	-1.0	-1.1	-1.9	-1.5	-1.8	-5.3	-2.8
N440K	-1.4	-1.4	-1.6	-1.2	-1.7	-1.4	-1.4	-1.6	-246	-1.5	-2.3	-18	-1.6	1.1	-2.0	-1.3	-1.5	-4.3	-2.8
G446S	1.3	1.1	-1.1	1.2	-1.6	-1.1	-1.6	-3.0	-574	-3.7	-1.7	-50	-1.4	-1.6	-2.2	-1.4	-2.2	-3.9	-2.4
S477N	-1.8	-1.8	-1.7	-1.7	-2.4	-1.5	-1.5	-1.7	-2.9	-1.6	-1.9	-4.4	-2.4	-1.5	-2.3	-1.6	-2.2	-17	-5.1
T478K	1.2	1.1	1.4	1.6	1.3	-1.5	-1.4	-1.2	-1.6	1.1	-1.8	-2.6	-1.6	-1.2	-2.8	-1.3	-2.3	-3.3	-2.3
E484A	-2.8	-1.7	-1.8	-1.2	-4.8	-4.9	<-1000	<-1000	-1.6	-1.4	-1.4	-2.7	-1.9	-1.6	-1.5	-1.9	-1.9	-5.7	-2.9
Q493R	-16	-7.3	-3.2	2.9	-42	-4.2	<-1000	-705	-1.4	-1.1	-1.2	-1.9	-2.0	-1.6	-1.6	-1.6	-1.5	-4.0	-1.3
G496S	-1.3	1.3	1.1	1.1	1.0	1.1	1.0	-9.3	-6.2	-1.3	-1.4	1.4	-1.2	-1.2	-1.6	-1.1	-1.6	-2.6	-1.6
Q498R	-1.7	-1.2	1.1	1.4	-1.5	-1.1	-1.4	-1.0	-1.6	-1.4	-1.3	1.1	-1.2	2.4	-1.3	-1.2	-1.3	-1.5	-1.8
N501Y	-9.8	-1.2	-8.4	-16	-1.4	-1.5	-1.6	-1.2	-1.2	-1.1	-1.8	-1.5	-2.7	-1.8	-2.5	-1.9	-1.9	-20	-3.9
Y505H	-1.2	1.2	-1.3	-9.6	1.1	1.0	1.0	1.1	1.4	1.0	-1.4	1.7	1.1	1.3	-1.4	1.0	-1.2	-1.2	-1.1
T547K	-1.9	-2.0	-2.0	-1.9	-1.7	-1.3	-1.6	-1.7	-2.7	-1.6	-1.6	-4.3	-1.9	-1.7	-2.6	-1.5	-1.9	-2.7	-2.7
H655Y	-2.7	-3.1	-3.5	-2.7	-3.1	-2.0	-2.2	-8.6	-8.8	-1.7	-2.3	-13	-2.4	-2.1	-3.9	-3.3	-3.9	-23	-5.3
N679K	1.0	1.2	1.1	1.1	-1.1	-1.2	-1.2	-1.2	-1.9	-1.1	-1.3	-1.8	-1.7	-1.4	-2.4	-1.7	-1.7	-2.1	-2.7
P681H	-2.3	-2.1	-2.1	1.0	-2.4	-1.8	-2.2	-1.5	-1.5	-1.0	-1.6	-1.9	-1.5	-1.3	-2.3	-1.3	-1.3	-2.3	-2.4
N764K	-1.1	-1.5	-1.3	-1.1	-1.4	-1.4	-1.4	-2.1	-2.5	-1.5	-2.2	-4.3	-1.3	-1.4	-3.3	-2.1	-2.4	-2.3	-2.1
D769Y	1.3	1.1	1.0	1.2	-1.5	-1.0	-1.4	-1.4	-2.0	-1.3	-1.9	-2.5	-1.3	-1.1	-1.7	-1.2	-1.4	-3.1	-2.5
N856K	-10	-2.8	-1.3	-12	-2.2	-3.0	-1.1	-1.0	-1.4	-1.1	-1.2	-1.3	-2.3	-1.8	-4.4	-2.1	-2.5	-1.6	-1.9
Q954H	2.7	1.9	1.5	2.6	1.2	1.0	1.2	1.1	-1.1	1.2	-1.2	-1.4	-1.1	-1.1	-2.5	-1.0	-1.1	-2.3	-2.9
N969K	-5.4	-1.6	-1.1	-4.5	-1.3	-1.8	-1.1	-1.3	-1.6	-1.1	-1.4	-2.4	-1.4	-1.1	-2.3	-2.0	-2.4	-2.5	-2.0
L981F	3.2	3.3	2.1	4.6	2.4	2.5	2.2	1.9	1.3	2.5	-1.0	-1.5	8.6	2.8	1.1	2.0	2.1	-1.3	-1.5

Legend: >3 | <-3 | <-10 | <-100

b

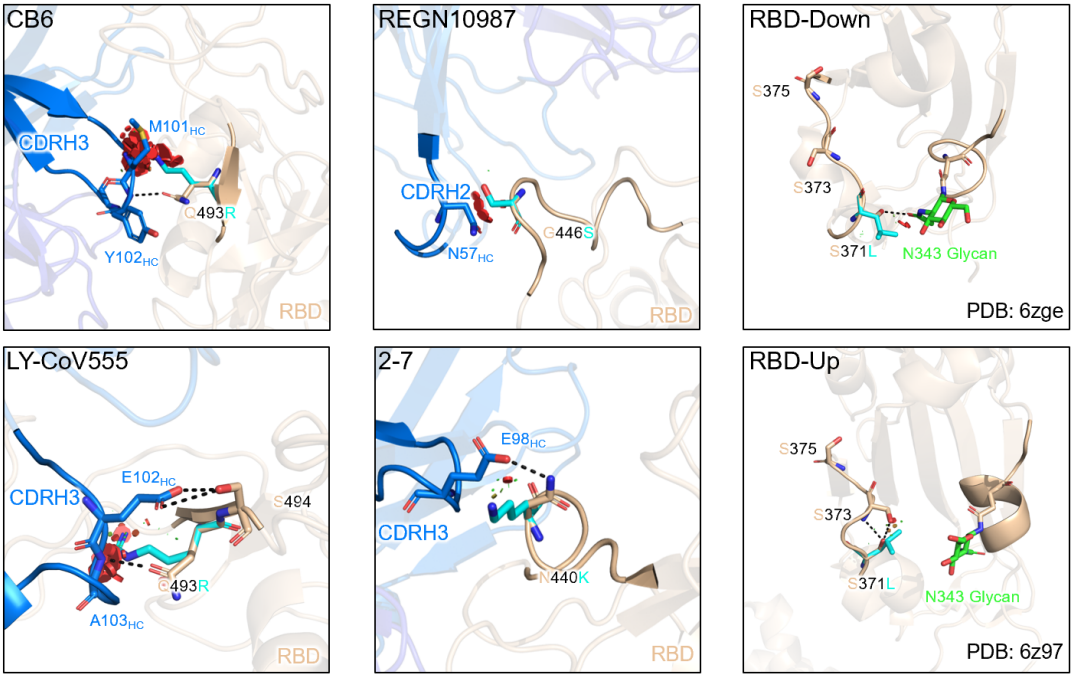

Fig. 4

Fold change in IC50 compared with WT	RBD mAbs																	NTD mAbs	
	Class 1				Class 2				Class 3					Class 4					
	CB6	Brii-196	1-20	910-30	REGN10933	COV2-2196	LY-CoV555	2-15	REGN10987	COV2-2130	S309	2-7	Brii-198	ADG-2	DH1047	10-40	S2X259	4-18	5-7
B.1.1.7	-8.8	2.6	-5.2	-15	1.6	1.8	1.6	2.2	2.9	1.7	1.1	2.3	4.1	1.7	2.2	1.4	1.4	-5.1	-4.0
B.1.526	-1.0	1.1	-1.1	2.5	-4.5	-2.1	-590	-1329	1.8	1.2	2.9	1.8	-1.1	1.5	2.9	-2.2	1.4	4.5	-2.5
B.1.429	3.0	2.3	1.4	2.5	2.5	2.8	-590	-4.6	1.6	1.1	1.9	1.6	-2.4	2.0	2.9	1.3	3.3	-39	-59
B.1.617.2	2.1	1.2	-1.1	2.5	1.2	1.4	-590	-10	-1.8	-1.7	1.2	-1.1	-8.9	1.0	1.4	-1.8	-1.4	-39	-74
P.1	-196	2.2	-16	-60	-121	-2.0	-590	-1329	1.9	1.1	1.1	1.2	1.8	-1.0	3.0	-2.2	1.2	-39	-74
B.1.351	-196	2.0	-40	-60	-78	-2.5	-590	-1329	1.5	1.5	1.2	1.9	-1.5	1.0	3.0	-2.9	1.2	-39	-8.4
B.1.1.529	<-1000	-134	<-338	<-159	<-1000	-140	<-1000	<-1000	<-1000	-390	-6.1	-231	2.2	-43	-124	-11	-35	-125	-30
B.1.1.529 + R346K	<-761	-97	<-338	<-159	<-1000	-89	<-1000	<-1000	<-1000	<-988	-21	-109	<-32	-51	-167	-32	-16	-125	-33

233

Legend: >3 | <-3 | <-10 | <-100

234 **References**

235

236 1 Shu, Y. & McCauley, J. GISAID: Global initiative on sharing all influenza data - from
237 vision to reality. *Euro Surveill* **22**, doi:10.2807/1560-7917.ES.2017.22.13.30494 (2017).
238 2 Grabowski, F., Kochańczyk, M. & Lipniacki, T. Omicron strain spreads with the
239 doubling time of 3.2—3.6 days in South Africa province of Gauteng that achieved herd
240 immunity to Delta variant. *medRxiv*, doi:https://doi.org/10.1101/2021.12.08.21267494
241 (2021).
242 3 Scott, L. *et al.* Track Omicron's spread with molecular data. *Science*, eabn4543,
243 doi:10.1126/science.abn4543 (2021).
244 4 Wang, P. *et al.* Antibody resistance of SARS-CoV-2 variants B.1.351 and B.1.1.7.
245 *Nature* **593**, 130-135, doi:10.1038/s41586-021-03398-2 (2021).
246 5 Abu-Raddad, L. J., Chemaitelly, H., Butt, A. A. & National Study Group for, C.-V.
247 Effectiveness of the BNT162b2 Covid-19 Vaccine against the B.1.1.7 and B.1.351
248 Variants. *N Engl J Med* **385**, 187-189, doi:10.1056/NEJMc2104974 (2021).
249 6 Madhi, S. A. *et al.* Efficacy of the ChAdOx1 nCoV-19 Covid-19 Vaccine against the
250 B.1.351 Variant. *N Engl J Med* **384**, 1885-1898, doi:10.1056/NEJMoa2102214 (2021).
251 7 Sadoff, J. *et al.* Safety and Efficacy of Single-Dose Ad26.COV2.S Vaccine against
252 Covid-19. *N Engl J Med* **384**, 2187-2201, doi:10.1056/NEJMoa2101544 (2021).
253 8 Davies, N. G. *et al.* Estimated transmissibility and impact of SARS-CoV-2 lineage
254 B.1.1.7 in England. *Science* **372**, doi:10.1126/science.abg3055 (2021).
255 9 Mlcochova, P. *et al.* SARS-CoV-2 B.1.617.2 Delta variant replication and immune
256 evasion. *Nature* **599**, 114-119, doi:10.1038/s41586-021-03944-y (2021).
257 10 Hadfield, J. *et al.* Nextstrain: real-time tracking of pathogen evolution. *Bioinformatics* **34**,
258 4121-4123, doi:10.1093/bioinformatics/bty407 (2018).
259 11 Pulliam, J. R. C. *et al.* Increased risk of SARS-CoV-2 reinfection associated with
260 emergence of the Omicron variant in South Africa. *medRxiv*,
261 doi:https://doi.org/10.1101/2021.11.11.21266068 (2021).
262 12 Hansen, J. *et al.* Studies in humanized mice and convalescent humans yield a SARS-
263 CoV-2 antibody cocktail. *Science* **369**, 1010-1014, doi:10.1126/science.abd0827 (2020).

264 13 Zost, S. J. *et al.* Potently neutralizing and protective human antibodies against SARS-
265 CoV-2. *Nature* **584**, 443-449, doi:10.1038/s41586-020-2548-6 (2020).
266 14 Jones, B. E. *et al.* The neutralizing antibody, LY-CoV555, protects against SARS-CoV-2
267 infection in nonhuman primates. *Sci Transl Med* **13**, doi:10.1126/scitranslmed.abf1906
268 (2021).
269 15 Shi, R. *et al.* A human neutralizing antibody targets the receptor-binding site of SARS-
270 CoV-2. *Nature* **584**, 120-124, doi:10.1038/s41586-020-2381-y (2020).
271 16 Ju, B. *et al.* Human neutralizing antibodies elicited by SARS-CoV-2 infection. *Nature*
272 **584**, 115-119, doi:10.1038/s41586-020-2380-z (2020).
273 17 Pinto, D. *et al.* Cross-neutralization of SARS-CoV-2 by a human monoclonal SARS-CoV
274 antibody. *Nature* **583**, 290-295, doi:10.1038/s41586-020-2349-y (2020).
275 18 Banach, B. B. *et al.* Paired heavy- and light-chain signatures contribute to potent SARS-
276 CoV-2 neutralization in public antibody responses. *Cell Rep* **37**, 109771,
277 doi:10.1016/j.celrep.2021.109771 (2021).
278 19 Rappazzo, C. G. *et al.* Broad and potent activity against SARS-like viruses by an
279 engineered human monoclonal antibody. *Science* **371**, 823-829,
280 doi:10.1126/science.abf4830 (2021).
281 20 Li, D. *et al.* In vitro and in vivo functions of SARS-CoV-2 infection-enhancing and
282 neutralizing antibodies. *Cell* **184**, 4203-4219 e4232, doi:10.1016/j.cell.2021.06.021
283 (2021).
284 21 Tortorici, M. A. *et al.* Broad sarbecovirus neutralization by a human monoclonal
285 antibody. *Nature* **597**, 103-108, doi:10.1038/s41586-021-03817-4 (2021).
286 22 Liu, L. *et al.* Potent neutralizing antibodies against multiple epitopes on SARS-CoV-2
287 spike. *Nature* **584**, 450-456, doi:10.1038/s41586-020-2571-7 (2020).
288 23 Cerutti, G. *et al.* Neutralizing antibody 5-7 defines a distinct site of vulnerability in
289 SARS-CoV-2 spike N-terminal domain. *Cell Rep* **37**, 109928,
290 doi:10.1016/j.celrep.2021.109928 (2021).
291 24 Liu, L. *et al.* Isolation and comparative analysis of antibodies that broadly neutralize
292 sarbecoviruses. *bioRxiv*, doi:https://doi.org/10.1101/2021.12.11.472236 (2021).
293 25 Barnes, C. O. *et al.* SARS-CoV-2 neutralizing antibody structures inform therapeutic
294 strategies. *Nature* **588**, 682-687, doi:10.1038/s41586-020-2852-1 (2020).

295 26 Cerutti, G. *et al.* Potent SARS-CoV-2 neutralizing antibodies directed against spike N-
296 terminal domain target a single supersite. *Cell Host Microbe* **29**, 819-833 e817,
297 doi:10.1016/j.chom.2021.03.005 (2021).
298 27 Uriu, K. *et al.* Neutralization of the SARS-CoV-2 Mu Variant by Convalescent and
299 Vaccine Serum. *N Engl J Med*, doi:10.1056/NEJMc2114706 (2021).
300 28 Annavajhala, M. K. *et al.* Emergence and expansion of SARS-CoV-2 B.1.526 after
301 identification in New York. *Nature* **597**, 703-708, doi:10.1038/s41586-021-03908-2
302 (2021).
303 29 Zhang, W. *et al.* Emergence of a Novel SARS-CoV-2 Variant in Southern California.
304 *JAMA* **325**, 1324-1326, doi:10.1001/jama.2021.1612 (2021).
305 30 Faria, N. R. *et al.* Genomics and epidemiology of the P.1 SARS-CoV-2 lineage in
306 Manaus, Brazil. *Science* **372**, 815-821, doi:10.1126/science.abh2644 (2021).
307 31 Tegally, H. *et al.* Detection of a SARS-CoV-2 variant of concern in South Africa. *Nature*
308 **592**, 438-443, doi:10.1038/s41586-021-03402-9 (2021).
309 32 Andrews, N. *et al.* Effectiveness of COVID-19 vaccines against the Omicron (B.1.1.529)
310 variant of concern. *medRxiv*, doi:https://doi.org/10.1101/2021.12.14.21267615 (2021).
311 33 Wroughton, L. in *The Washington Post* (2021).
312 34 Kuhlmann, C. *et al.* Breakthrough Infections with SARS-CoV-2 Omicron Variant
313 Despite Booster Dose of mRNA Vaccine. *SSRN*,
314 doi:https://dx.doi.org/10.2139/ssrn.3981711 (2021).
315 35 Garcia-Beltran, W. F. *et al.* mRNA-based COVID-19 vaccine boosters induce
316 neutralizing immunity against SARS-CoV-2 Omicron variant. *medRxiv*,
317 doi:https://doi.org/10.1101/2021.12.14.21267755 (2021).
318 36 Cromer, D. *et al.* Neutralising antibody titres as predictors of protection against SARS-
319 CoV-2 variants and the impact of boosting: a meta-analysis. *Lancet Microbe*,
320 doi:10.1016/S2666-5247(21)00267-6 (2021).
321 37 Baym, M. *et al.* Inexpensive multiplexed library preparation for megabase-sized
322 genomes. *PLoS One* **10**, e0128036, doi:10.1371/journal.pone.0128036 (2015).
323 38 Martin, M. Cutadapt Removes Adapter Sequences From High-Throughput Sequencing
324 Reads. *EMBnet.journal* **17**, 10, doi:10.14806/ej.17.1.200 (2011).

325 39 Langmead, B. & Salzberg, S. L. Fast gapped-read alignment with Bowtie 2. *Nat Methods*
326 **9**, 357-359, doi:10.1038/nmeth.1923 (2012).
327 40 Robinson, J. T. *et al.* Integrative genomics viewer. *Nat Biotechnol* **29**, 24-26,
328 doi:10.1038/nbt.1754 (2011).
329 41 Chu, H. *et al.* Comparative tropism, replication kinetics, and cell damage profiling of
330 SARS-CoV-2 and SARS-CoV with implications for clinical manifestations,
331 transmissibility, and laboratory studies of COVID-19: an observational study. *Lancet*
332 *Microbe* **1**, e14-e23, doi:10.1016/S2666-5247(20)30004-5 (2020).
333 42 Krissinel, E. & Henrick, K. Inference of macromolecular assemblies from crystalline
334 state. *J Mol Biol* **372**, 774-797, doi:10.1016/j.jmb.2007.05.022 (2007).
335

336 **Methods**

337

338 **Serum samples**

339 Convalescent plasma samples were obtained from patients with documented SARS-CoV-2
340 infection approximately one month after recovery or later. These samples were collected at the
341 beginning of the pandemic in early 2020 at Columbia University Irving Medical Center, and
342 therefore are assumed to be infection by the wild-type strain of SARS-CoV-2[4]. Sera from
343 individuals who received two or three doses of mRNA-1273 or BNT162b2 vaccine were collected
344 at Columbia University Irving Medical Center at least two weeks after the final dose. Sera from
345 individuals who received one dose of Ad26.COV2.S or two doses of ChAdOx1 nCov-19 were
346 obtained from BEI Resources. Some individuals were also infected by SARS-CoV-2 in addition
347 to the vaccinations they received. Note that, whenever possible, we specifically chose samples
348 with high titers against the wild-type strain of SARS-CoV-2 such that the loss in activity against
349 B.1.1.529 could be better quantified, and therefore the titers observed here should be considered
350 in that context. All collections were conducted under protocols reviewed and approved by the
351 Institutional Review Board of Columbia University. Additional information for the vaccinee
352 samples can be found in **Extended Data Table 1**.

353

354 **Monoclonal antibodies**

355 Antibodies were expressed as previously described[22], by synthesis of VH and VL genes
356 (GenScript), transfection of Expi293 cells (Thermo Fisher), and affinity purification from the
357 supernatant by rProtein A Sepharose (GE). REGN10987, REGN10933, COV2-2196, and COV2-
358 2130 were provided by Regeneron Pharmaceuticals, Brii-196 and Brii-198 were provided by Brii
359 Biosciences, CB6 was provided by Baoshan Zhang and Peter Kwong (NIH), and 910-30 was
360 provided by Brandon DeKosky (MIT).

361

362 **Variant SARS-CoV-2 spike plasmid construction**

363 An in-house high-throughput template-guide gene synthesis approach was used to generate spike
364 genes with single or full mutations of B.1.1.529. Briefly, 5'-phosphorylated oligos with designed
365 mutations were annealed to the reverse strand of the wild-type spike gene construct and extended
366 by DNA polymerase. Extension products (forward-stranded fragments) were then ligated together

367 by Taq DNA ligase and subsequently amplified by PCR to generate variants of interest. To verify
368 the sequences of variants, NGS libraries were prepared following a low-volume Nextera
369 sequencing protocol[37] and sequenced on the Illumina Miseq platform (single-end mode with 50 bp
370 R1). Raw reads were processed by Cutadapt v2.1[38] with default setting to remove adapters and
371 then aligned to reference variants sequences using Bowtie2 v2.3.4[39] with default setting. Resulting
372 reads alignments were then visualized in Integrative Genomics Viewer[40] and subjected to manual
373 inspection to verify the fidelity of variants. Sequences of the oligos used in variants generation are
374 provided in **Extended Data Table 2**.
375
376 **Pseudovirus production**
377 Pseudoviruses were produced in the vesicular stomatitis virus (VSV) background, in which the
378 native glycoprotein was replaced by that of SARS-CoV-2 and its variants, as previously
379 described[24]. Briefly, HEK293T cells were transfected with a spike expression construct with PEI
380 (1 mg/mL) and cultured overnight at 37 °C under 5% CO_2, and then infected with VSV-G
381 pseudotyped ΔG-luciferase (G*ΔG-luciferase, Kerafast) one day post-transfection. Following 2 h
382 of infection, cells were washed three times, changed to fresh medium, and then cultured for
383 approximately another 24 h before supernatants were collected, centrifuged, and aliquoted to use
384 in assays.
385
386 **Pseudovirus neutralization assay**
387 All viruses were first titrated to normalize the viral input between assays. Heat-inactivated sera or
388 antibodies were first serially diluted in 96 well-plates in triplicate. Viruses were then added and
389 the virus-sample mixture was incubated at 37 °C for 1 h. Vero-E6 cells (ATCC) were then added
390 at a density of 3×10^4 cells per well and plates were incubated at 37 °C for approximately 10 h.
391 Luciferase activity was quantified by using the Luciferase Assay System (Promega) according to
392 the manufacturer's instructions. Neutralization curves and IC_{50} values were derived by fitting a
393 non-linear five-parameter dose-response curve to the data in GraphPad Prism version 9.2.
394
395 **Authentic virus isolation and propagation**
396 Authentic B.1.1.529 was isolated from a specimen from the respiratory tract of a COVID-19
397 patient in Hong Kong by Kwok-Yung Yuen and colleagues at the Department of Microbiology,

398 The University of Hong Kong. Isolation of wild-type SARS-CoV-2 was previously described[41].
399 Viruses were propagated in Vero-E6-TMPRSS2 cells and sequence confirmed by next-generation
400 sequencing prior to use.
401
402 **Authentic virus neutralization assay**
403 To measure neutralization of authentic SARS-CoV-2 viruses, Vero-E6-TMPRSS2 cells were first
404 seeded in 96 well-plates in cell culture media (DMEM + 10% FBS + 1% penicillin/streptomycin)
405 overnight at 37 °C under 5% CO_2 to establish a monolayer. The following day, sera or antibodies
406 were serially diluted in 96 well-plates in triplicate in DMEM + 2% FBS and then incubated with
407 0.01 MOI of wild-type SARS-CoV-2 or B.1.1.529 at 37 °C for 1 h. Afterwards, the mixture was
408 overlaid onto cells and further incubated at 37 °C under 5% CO_2 for approximately 72 h.
409 Cytopathic effects were then visually assessed in all wells and scored as either negative or positive
410 for infection by comparison to control uninfected or infected wells in a blinded manner.
411 Neutralization curves and IC_{50} values were derived by fitting a non-linear five-parameter dose-
412 response curve to the data in GraphPad Prism version 9.2.
413
414 **Antibody footprint analysis and RBD mutagenesis analysis**
415 The SARS-CoV-2 spike structure used for displaying epitope footprints and mutations within
416 emerging strains was downloaded from PDB (PDBID: 6ZGE). The structures of antibody-spike
417 complexes were also obtained from PDB (7L5B for 2-15, 6XDG for REGN10933 and
418 REGN10987, 7L2E for 4-18, 7RW2 for 5-7, 7C01 for CB6, 7KMG for LY-COV555, 7CDI for
419 Brii-196, 7KS9 for 910-30, 7LD1 for DH1047, 7RAL for S2X259, 7LSS for 2-7, and 6WPT for
420 S309). Interface residues were identified using PISA[42] using default parameters. The footprint for
421 each antibody was defined by the boundaries of all epitope residues. The border for each footprint
422 was then optimized by ImageMagick 7.0.10-31 (https://imagemagick.org). PyMOL 2.3.2 was used
423 to perform mutagenesis and to make structural plots (Schrödinger).
424

Acknowledgements

We are grateful Regeneron Pharmaceuticals, B. Zhang and P. Kwong (NIAID), and B. Dekosky (MIT) for antibodies. This study was supported by funding from the Gates Foundation, JPB Foundation, Andrew and Peggy Cherng, Samuel Yin, Carol Ludwig, David and Roger Wu, Health@InnoHK, and the National Science Foundation (MCB-2032259).

Author contributions

D.D.H. conceived this project. L.H.L., S.I., and M.W. conducted pseudovirus neutralization experiments. J.F-W.C., H.C., K.K-H.C., T.T-T.Y., C.Y., K.K-W.T., and H.C. conducted authentic virus neutralization experiments. Y.G. and Z.Z. conducted bioinformatic analyses. L.Y.L. and Y.M.H. constructed the spike expression plasmids. Y.L. managed the project. J.Y. expressed and purified antibodies. M.T.Y. and M.E.S. provided clinical samples. M.S.N. and Y.X.H. contributed to discussions. H.H.W., K-Y.Y., and D.D.H. directed and supervised the project. L.H.L., S.I., and D.D.H. analyzed the results and wrote the manuscript.

Competing interests

L.L., S.I., M.S.N., J.Y., Y.H., and D.D.H. are inventors on patent applications on some of the antibodies described in this manuscript.

Data and materials availability

All data are provided in the paper or the Supplementary Information.